LETTERS

Quantum oscillations and the Fermi surface in an underdoped high-T_c superconductor

Nicolas Doiron-Leyraud[1], Cyril Proust[2], David LeBoeuf[1], Julien Levallois[2], Jean-Baptiste Bonnemaison[1], Ruixing Liang[3,4], D. A. Bonn[3,4], W. N. Hardy[3,4] & Louis Taillefer[1,4]

Despite twenty years of research, the phase diagram of high-transition-temperature superconductors remains enigmatic[1,2]. A central issue is the origin of the differences in the physical properties of these copper oxides doped to opposite sides of the superconducting region. In the overdoped regime, the material behaves as a reasonably conventional metal, with a large Fermi surface[3,4]. The underdoped regime, however, is highly anomalous and appears to have no coherent Fermi surface, but only disconnected 'Fermi arcs'[5,6]. The fundamental question, then, is whether underdoped copper oxides have a Fermi surface, and if so, whether it is topologically different from that seen in the overdoped regime. Here we report the observation of quantum oscillations in the electrical resistance of the oxygen-ordered copper oxide $YBa_2Cu_3O_{6.5}$, establishing the existence of a well-defined Fermi surface in the ground state of underdoped copper oxides, once superconductivity is suppressed by a magnetic field. The low oscillation frequency reveals a Fermi surface made of small pockets, in contrast to the large cylinder characteristic of the overdoped regime. Two possible interpretations are discussed: either a small pocket is part of the band structure specific to $YBa_2Cu_3O_{6.5}$ or small pockets arise from a topological change at a critical point in the phase diagram. Our understanding of high-transition-temperature (high-T_c) superconductors will depend critically on which of these two interpretations proves to be correct.

The electrical resistance of two samples of ortho-II ordered $YBa_2Cu_3O_{6.5}$ was measured in a magnetic field of up to 62 T applied normal to the CuO_2 planes ($B||c$). (Sample characteristics and details of the measurements are given in the Methods section.) With a T_c of 57.5 K, these samples have a hole doping per planar copper atom of $p = 0.10$, that is, they are well into the underdoped region of the phase diagram (see Fig. 1a). Angle-resolved photoemission spectroscopy (ARPES) data for underdoped $Na_{2-x}Ca_xCu_2O_2Cl_2$ (Na-CCOC) at precisely the same doping (reproduced in Fig. 1b from ref. 6) shows most of the spectral intensity to be concentrated in a small region near the nodal position ($\pi/2$, $\pi/2$), suggesting a Fermi surface broken up into disconnected arcs, while ARPES studies on overdoped $Tl_2Ba_2CuO_{6+\delta}$ (Tl-2201) at $p = 0.25$ reveal a large, continuous cylinder (reproduced in Fig. 1c from ref. 4).

The Hall resistance R_{xy} as a function of magnetic field is displayed in Fig. 2 for sample A, and in Supplementary Fig. 1 for sample B, where oscillations are clearly seen above the resistive superconducting transition. Note that a vortex liquid phase is believed to extend well above the irreversibility field, beyond our highest field of 62 T, which may explain why R_{xy} is negative at these low temperatures, as opposed to positive at temperatures above T_c. Nevertheless, quantum oscillations are known to exhibit the very same diagnostic characteristics of frequency and mass in the vortex state as in the field-induced normal state above the upper critical field $H_{c2}(0)$ (for example, ref. 7). They are caused by the passage of quantized Landau levels across the Fermi level as the applied magnetic field is varied, and as such they are considered the most robust and direct signature of a coherent Fermi surface. The inset of Fig. 2 shows the 2 K isotherm and a smooth background curve. We extract the oscillatory component, plotted in Fig. 3a as a function

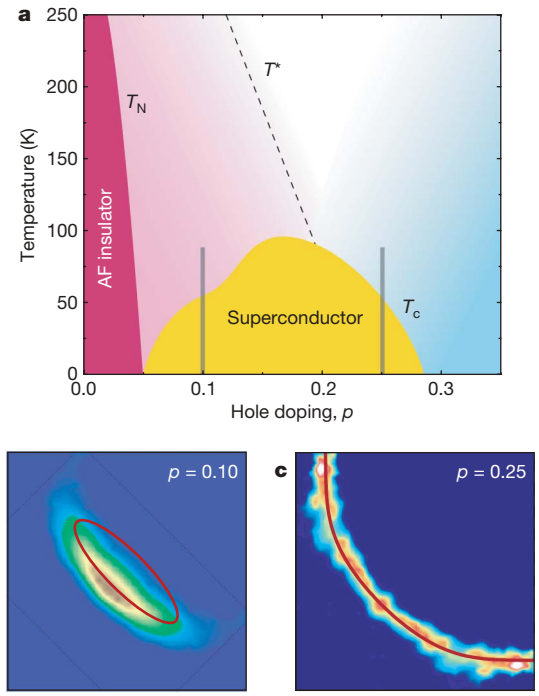

Figure 1 | Phase diagram of high-temperature superconductors. **a**, Schematic doping dependence of the antiferromagnetic (T_N) and superconducting (T_c) transition temperatures and the pseudogap crossover temperature T^* in YBCO. The vertical lines at $p = 0.1$ and $p = 0.25$ mark the positions of copper oxide materials discussed in the text: ortho-II ordered $YBa_2Cu_3O_{6.5}$ and Na-CCOC, located well into the underdoped region, and Tl-2201, well into the overdoped region, respectively. **b**, **c**, Distribution of ARPES spectral intensity in one quadrant of the Brillouin zone, measured (**b**), on Na-CCOC at $p = 0.1$, and (**c**), on Tl-2201 at $p = 0.25$ (reproduced from ref. 6 and ref. 4, with permissions from K. M. Shen and A. Damascelli, respectively). These respectively reveal a truncated Fermi surface made of 'Fermi arcs' at $p = 0.10$, and a large, roughly cylindrical and continuous Fermi surface at $p = 0.25$. The red ellipse in **b** encloses an area A_k that corresponds to the frequency F of quantum oscillations measured in YBCO.

[1]Département de physique and RQMP, Université de Sherbrooke, Sherbrooke, Canada J1K 2R1. [2]Laboratoire National des Champs Magnétiques Pulsés (LNCMP), UMR CNRS-UPS-INSA 5147, Toulouse 31400, France. [3]Department of Physics and Astronomy, University of British Columbia, Vancouver, Canada V6T 1Z4. [4]Canadian Institute for Advanced Research, Toronto, Canada M5G 1Z8.

of inverse field, by subtracting the monotonic background (shown for all temperatures in Supplementary Fig. 2). This shows that the oscillations are periodic in $1/B$, as is expected of oscillations that arise from Landau quantization. A Fourier transform yields the power spectrum, displayed in Fig. 3b, which consists of a single frequency, $F = (530 \pm 20)$ T. In Fig. 3c, we plot the amplitude of the oscillations as a function of temperature, from which we deduce a carrier mass $m^* = (1.9 \pm 0.1)m_0$, where m_0 is the bare electron mass. Within error bars, both F and m^* are the same in sample B, for which the current J is parallel to the b axis (see Supplementary Fig. 1). Oscillations of the same frequency are also observed in R_{xx} (in both samples), albeit with a smaller amplitude. We note that while at 7.5 K the oscillations are still perceptible, they are absent at 11 K, as expected from thermally damped quantum oscillations (see Supplementary Fig. 5).

While quantum oscillations in $YBa_2Cu_3O_{6+y}$ (YBCO) have been the subject of a number of earlier studies[8–10], the data reported so far do not exhibit clear oscillations as a function of $1/B$ and, as such, have not been accepted as convincing evidence for a Fermi surface[11]. Furthermore, we note that all previous work was done on oriented powder samples as opposed to the high-quality single crystals used in the present study.

Quantum oscillations are a direct measure of the Fermi surface area via the Onsager relation: $F = (\Phi_0/2\pi^2)A_k$, where $\Phi_0 = (2.07 \times 10^{-15})$ T m^2 is the flux quantum, and A_k is the cross-sectional area of the Fermi surface normal to the applied field. A frequency of 530 T implies a Fermi surface pocket that encloses a k-space area (in the a–b plane) of $A_k = 5.1$ nm^{-2}, that is, 1.9% of the Brillouin zone (of area $4\pi^2/ab$). This is only 3% of the area of the Fermi surface cylinder measured in Tl-2201 (see Fig. 1c), whose radius is $k_F \approx 7$ nm^{-1}. In the remainder, we examine two scenarios to explain the dramatic difference between the small Fermi surface revealed by the low frequency of quantum oscillations reported here for $YBa_2Cu_3O_{6.5}$ and the large cylindrical surface observed in overdoped Tl-2201. The first scenario assumes that the particular band structure of $YBa_2Cu_3O_{6.5}$ is different and supports a small Fermi surface sheet. In the second, the electronic structure of overdoped copper oxides undergoes a transformation as the doping p is reduced below a value p_c associated with a critical point.

Band structure calculations for stoichiometric YBCO ($y = 1.0$), which is slightly overdoped (with $p = 0.2$), show a Fermi surface consisting of four sheets[12,13], as reproduced in Fig. 4a: two large cylinders derived from the CuO_2 bi-layer, one open surface coming from the CuO chains, and a small cylinder associated with both chain and plane states. The latter sheet, for example, could account for the low frequency reported here. ARPES studies on YBCO near optimal doping[14,15] appear to be in broad agreement with this electronic structure. However, recent band structure calculations[16] performed specifically for $YBa_2Cu_3O_{6.5}$, which take into account the unit cell doubling caused by the ortho-II order, give a Fermi surface where the small cylinder is absent, as shown in Fig. 4b. This leaves no obvious candidate Fermi surface sheet for the small orbit reported here.

The fact that the same oscillations are observed for currents along a and b suggests that they are not associated with open orbits in the chain-derived Fermi surface sheet. In YBCO, the CuO chains along the b axis are an additional channel of conduction, responsible for an anisotropy in the zero-field resistivity $\rho(T)$ of the normal state (above

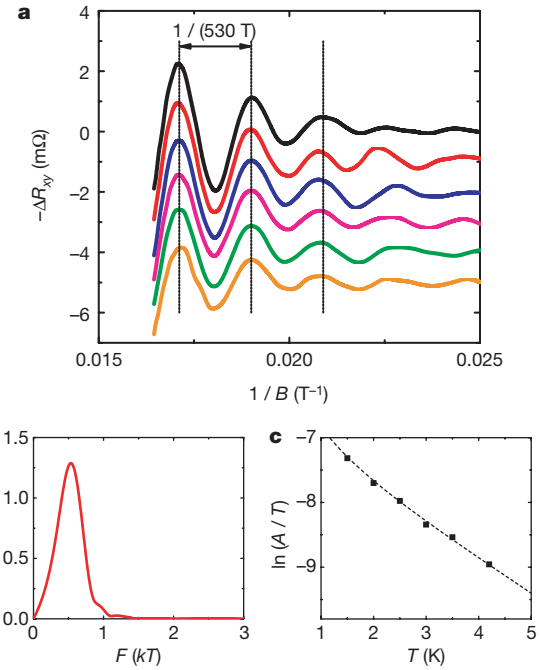

Figure 3 | Quantum oscillations in YBCO. **a**, Oscillatory part of the Hall resistance, obtained by subtracting the monotonic background (shown in the inset of Fig. 2 for $T = 2$ K), as a function of inverse magnetic field, $1/B$. The background at each temperature is given in Supplementary Fig. 2. **b**, Power spectrum (Fourier transform) of the oscillatory part for the $T = 2$ K isotherm, revealing a single frequency at $F = (530 \pm 20)$ T, which corresponds to a k-space area $A_k = 5.1$ nm^{-2}, from the Onsager relation $F = (\Phi_0/2\pi^2)A_k$. Note that the uncertainty of 4% on F is not given by the width of the peak (a consequence of the small number of oscillations), but by the accuracy with which the position of successive maxima in **a** can be determined. **c**, Temperature dependence of the oscillation amplitude A, plotted as $\ln(A/T)$ versus T. The fit is to the standard Lifshitz–Kosevich formula, whereby $A/T = [\sinh(am^*T/B)]^{-1}$, which yields a cyclotron mass $m^* = (1.9 \pm 0.1)m_0$, where m_0 is the free electron mass.

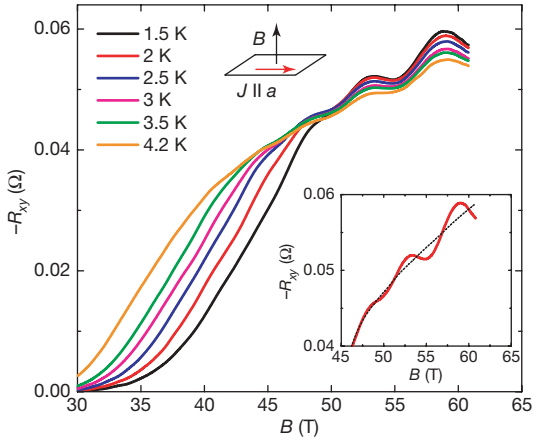

Figure 2 | Hall resistance of $YBa_2Cu_3O_{6.5}$. R_{xy} as a function of magnetic field B, for sample A, at different temperatures between 1.5 and 4.2 K. The field is applied normal to the CuO_2 planes ($B \| c$) and the current is along the a axis of the orthorhombic crystal structure ($J \| a$). The inset shows a zoom on the data at $T = 2$ K, with a fitted monotonic background (dashed line).

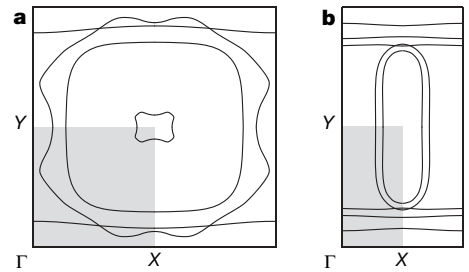

Figure 4 | Fermi surface of YBCO from band structure calculations. **a**, Fermi surface of $YBa_2Cu_3O_7$ in the $k_z = 0$ plane (from ref. 13, with permission from O. K. Andersen), showing the four bands discussed in the main text. **b**, Fermi surface of ortho-II ordered $YBa_2Cu_3O_{6.5}$ in the $k_z = 0$ plane (from ref. 16, with permission from T. M. Rice). In both **a** and **b** the grey shading indicates one quadrant of the first Brillouin zone.

T_c). In Supplementary Fig. 3, we plot the anisotropy ratio ρ_a/ρ_b as a function of temperature, and the chain resistivity versus T^2, obtained from samples A and B. Although the anisotropy is about 2.2 at 300 K, it eventually disappears as $T \rightarrow T_c$, with $\rho_a/\rho_b \approx 1.0$ for $T < 80$ K, owing to the localization of carriers in the quasi-one-dimensional chains. We thus conclude that chains make a negligible contribution to electrical transport at the low temperatures where quantum oscillations are observed. The oscillations must therefore come from the electronic structure of the CuO_2 planes.

The apparent lack of agreement between our experimental data and the calculated band structure of ortho-II $YBa_2Cu_3O_{6.5}$ calls for a careful re-examination of the band structure of YBCO near $p = 0.1$, both with and without ortho-II order. Let us then consider the possibility that electron correlations and/or the onset of an ordered phase with broken symmetry bring about a radical change in the Fermi surface from that predicted by local density approximation (LDA) calculations.

Much like in chromium where a spin-density-wave order causes the Fermi surface to reconstruct, a transformation in the electronic structure of YBCO could take place as a function of doping, resulting in small Fermi surface pockets. Such a scenario was invoked to explain the electron-doped copper oxides[17]. Comparison of A_k in YBCO with ARPES measurements[6] on Na-CCOC at the same doping ($p = 0.1$) suggests that the small Fermi surface pockets observed here are centred at nodal positions, that is to say at the crossing of the original large Fermi surface cylinder with the diagonal from (0, 0) to (π, π), that is near ($\pi/2$, $\pi/2$). In Fig. 1b, we show how an elliptical Fermi surface pocket with an area of 5 nm^{-2} located at this position would indeed match the ARPES spectral weight. Extending this to the four nodal positions could be a solution to the intriguing problem of the 'Fermi arcs', revealing them to be elongated Fermi pockets. Let us examine some implications of this four-pocket scenario.

Assuming that the Fermi surface is strictly two-dimensional, that is, neglecting any c axis dispersion, then the carrier density n per plane per area is given by Luttinger's theorem as $n = 2A_k/(2\pi)^2 = F/\Phi_0$ for each pocket. For four pockets, this gives $n = 1.02\ nm^{-2} = 0.152 \pm 0.006$ carriers per planar Cu atom ($ab = (0.38227 \times 0.38872)\ nm^2$ is the area per Cu atom). Thus we find that $n/p = 1.5$. Taken literally, this would imply that the addition of one hole doped into the CuO_2 plane does not result in identically one extra charge carrier. Or, in other words, the Luttinger sum rule that relates the number of mobile carriers to the Fermi surface volume (or area in two dimensions) appears to be violated. This intriguing possibility depends on a number of assumptions that will require careful examination.

First, we assume that the Onsager relation applies in copper oxides exactly as it does in normal metals, that is, it is the frequency of oscillations in inverse applied magnetic field, rather than some other internal field, which is related to the Fermi surface area via $F = (\Phi_0/2\pi^2)A_k$. Second, we ignore the possibility that electron Fermi surface pockets may also exist, although it is not clear why they were not seen here. Finally, we neglect any dispersion along the c axis. However, to recover the Luttinger sum rule solely on this ground, a rather strong dispersion is necessary, something not predicted by band calculations nor evidenced by an additional quantum oscillation frequency.

For comparison, the carrier density in overdoped Tl-2201 at $p = 0.25$ is $n = (1.26 \pm 0.04)$ hole(s) per Cu atom, as obtained by the Hall effect[18], angular magnetoresistance oscillations (AMRO)[3] and ARPES[4]. In Fig. 1c, this is directly given by the measured Fermi surface area. This is precisely the value expected in the large-Fermi surface scenario of band theory, where $n = 1 + p$. Extending this down to $p = 0.1$ would predict that n should be 1.1 in $YBa_2Cu_3O_{6.5}$. The fact that we get $n = 0.15$ when we assume that the Fermi surface consists of no other sheet than the one manifest in the single frequency observed in our experiment means one of two things: either it is incorrect to extend the $n = 1 + p$ relation down into the underdoped regime, or large parts of the Fermi surface of YBCO were not seen in our experiment (possibly because of a much larger m^*).

In other words, in the four-nodal pocket scenario a transition between a large-Fermi surface metal (in the overdoped regime) and a small-Fermi surface metal (in the underdoped regime) occurs at a critical doping somewhere between $p = 0.1$ and $p = 0.25$. The associated drop in carrier density n by one order of magnitude would be expected to show up in most physical properties, for example the superfluid density n_S and the normal-state electronic specific heat coefficient γ_N. Assuming the dynamical mass $m_d^* \approx 2m_0$, close to the thermal mass m^* deduced from quantum oscillations, we get $n_S = m_d^* c^2/(4\pi e^2 \lambda^2) \approx 0.12$ carriers per planar Cu atom, from the experimentally measured in-plane penetration depth of ortho-II ordered YBCO: $\lambda_a = (200 \pm 20)$ nm (ref. 19). This low value of n_S is much closer to the carrier density obtained in the four-nodal-pocket scenario ($n = 0.15$) than in the large-Fermi-surface scenario ($n = 1 + p = 1.1$). Note, however, that a number of factors need to be considered carefully to make such a quantitative comparison compelling, including the real dynamical mass and the possibility of strong phase fluctuations. The loss in density of states that would follow a Fermi surface transformation into small pockets could also explain the large and sudden drop in γ_N that has been observed in various copper oxides as the doping is reduced below $p \approx 0.19$ (ref. 20).

A number of theories predict a Fermi surface made of four small pockets at nodal positions in the underdoped regime, going over to a large Fermi surface when p exceeds a critical value p_c. Some of these are analogous to the usual spin-density-wave scenario[17] in the sense that they invoke the onset of an ordered phase with broken symmetry below p_c (refs 21–23), while others do not require any broken symmetry[24–26].

In summary, our unambiguous observation of quantum oscillations in underdoped YBCO proves the existence of a Fermi surface. The small size of the Fermi surface pocket associated with the low oscillation frequency suggests two very different scenarios for the non-superconducting ground state of underdoped copper oxides. The first is a multi-band scenario in which the ground state is described by the LDA band structure. In the second scenario, the pseudogap phase that lies to the left of T^* in the phase diagram is a highly correlated electronic fluid with a Fermi surface made of small pockets at nodal positions, separated from the Fermi liquid of the overdoped regime by a critical point near optimal doping.

METHODS SUMMARY

Samples. The samples used are fully detwinned crystals of $YBa_2Cu_3O_{6+y}$ grown in non-reactive $BaZrO_3$ crucibles from high-purity starting materials (see ref. 27). The oxygen content was set at $y = 0.51$ and the dopant oxygen atoms were made to order into an ortho-II superstructure of alternating full and empty CuO_y chains, yielding a superconducting transition temperature $T_c = 57.5$ K. The samples are uncut, unpolished thin platelets, whose transport properties are measured via gold evaporated contacts (contact resistance $<1\ \Omega$), in a six-contact geometry. Sample A (current along a axis) and sample B (current along b axis) have dimensions ($40 \times 520 \times 720$) μm^3 (thickness × length × width) and ($65 \times 810 \times 1{,}030$) μm^3, respectively.

Estimates of hole doping. The hole doping p in YBCO is determined from a relationship between T_c and the c axis lattice constant (see ref. 28). For our samples, the measured $T_c = 57.5$ K implies $p = 0.099$ and the measured $c = (1.17441 \pm 0.00005)$ nm gives $p = 0.098 \pm 0.001$ (ref. 28).

Resistance measurements. Longitudinal (R_{xx}) and transverse (R_{xy}) resistances are obtained from the voltage difference measured diagonally on either side of the sample width, for a field parallel (up) and anti-parallel (down) to the c axis: $R_{xx} \equiv (V_{up} + V_{down})/2I_x$ and $R_{xy} \equiv (V_{up} - V_{down})/2I_x$. A current excitation of 5 mA at 40 kHz was used. The voltage (and a reference signal) was digitized using a high-speed digitizer and post-analysed to perform the phase comparison. The measurements were performed at the LNCMP in Toulouse, in a pulsed resistive magnet of up to 62 T (ref. 29). Data for the rise (26 ms) and fall (110 ms) of the field pulse were in perfect agreement, thus excluding any heating due to eddy current.

Received 3 April; accepted 18 April 2007.

1. Orenstein, J. & Millis, A. J. Advances in the physics of high-temperature superconductivity. *Science* **288,** 468–474 (2000).
2. Norman, M. R., Pines, D. & Kallin, C. The pseudogap: friend or foe of high T_c? *Adv. Phys.* **54,** 715–733 (2005).
3. Hussey, N. E. *et al.* Observation of a coherent three-dimensional Fermi surface in a high-transition temperature superconductor. *Nature* **425,** 814–817 (2003).
4. Platé, M. *et al.* Fermi surface and quasiparticle excitations of overdoped $Tl_2Ba_2CuO_{6+\delta}$ by ARPES. *Phys. Rev. Lett.* **95,** 077001 (2005).
5. Norman, M. *et al.* Destruction of the Fermi surface in underdoped high-T_c superconductors. *Nature* **392,** 157–160 (1998).
6. Shen, K. *et al.* Nodal quasiparticles and antinodal charge ordering in $Ca_{2-x}Na_xCuO_2Cl_2$. *Science* **307,** 901–904 (2005).
7. Wosnitza, J. *et al.* Shubnikov-de Haas effect in the superconducting state of an organic superconductor. *Phys. Rev. B* **62,** 11973–11976 (2000).
8. Fowler, C. M. *et al.* de Haas-van Alphen effect and Fermi surface of $YBa_2Cu_3O_{6.97}$. *Phys. Rev. Lett.* **68,** 534–537 (1992).
9. Kido, G., Komorita, K., Katayama-Yoshida, H. & Takahashi, T. de Haas-van Alphen measurement of $YBa_2Cu_3O_7$. *J. Phys. Chem. Solids* **52,** 1465–1470 (1991).
10. Haanappel, E. G. *et al.* The de Haas-van Alphen effect in $YBa_2Cu_3O_{7-\delta}$. *J. Phys. Chem. Solids* **54,** 1261–1267 (1993).
11. Springford, M., Harrison, N., Meeson, P. & Probst, P.-A. Comment on "de Haas-van Alphen effect and Fermi surface of $YBa_2Cu_3O_{6.97}$". *Phys. Rev. Lett.* **69,** 2453 (1992).
12. Pickett, W. E., Cohen, R. E. & Krakauer, H. Precise band structure and Fermi-surface calculation for $YBa_2Cu_3O_7$: Importance of three-dimensional dispersion. *Phys. Rev. B* **42,** 8764–8767 (1990).
13. Andersen, O. K., Liechtenstein, A. I., Jepsen, O. & Paulsen, F. LDA energy bands, low-energy Hamiltonians, t', t'', $t_\perp(\mathbf{k})$, and $J_\perp$. *J. Phys. Chem. Solids* **56,** 1573–1591 (1995).
14. Campuzano, J. C. *et al.* Fermi surfaces of $YBa_2Cu_3O_{6.9}$ as seen by angle-resolved photoemission. *Phys. Rev. Lett.* **64,** 2308–2311 (1990).
15. Nakayama, K. *et al.* Bulk and surface low-energy excitations in $YBa_2Cu_3O_{7-\delta}$ studied by high-resolution angle-resolved photoemission spectroscopy. *Phys. Rev. B* **75,** 014513 (2007).
16. Bascones, E. *et al.* Optical conductivity of ortho-II $YBa_2Cu_3O_{6.5}$. *Phys. Rev. B* **71,** 012505 (2005).
17. Lin, J. & Millis, A. J. Theory of low-temperature Hall effect in electron-doped cuprates. *Phys. Rev. B* **72,** 214506 (2005).
18. Mackenzie, A. P., Julian, S. R., Sinclair, D. C. & Lin, C. T. Normal-state magneto-transport in superconducting $Tl_2Ba_2CuO_{6+y}$ to millikelvin temperatures. *Phys. Rev. B* **53,** 5848–5855 (1996).
19. Pereg-Barnea, T. *et al.* Absolute values of the London penetration depth in $YBa_2Cu_3O_{6+y}$ measured by zero field ESR spectroscopy on Gd doped single crystals. *Phys. Rev. B* **69,** 184513 (2004).
20. Loram, J. W. *et al.* Specific heat evidence on the normal state pseudogap. *J. Phys. Chem. Solids* **59,** 2091–2094 (1998).
21. Chakravarty, S., Laughlin, R. B., Morr, D. K. & Nayak, C. Hidden order in the cuprates. *Phys. Rev. B* **63,** 094503 (2001).
22. Lee, P. A. & Wen, X.-G. Vortex structure in underdoped cuprates. *Phys. Rev. B* **63,** 224517 (2001).
23. Oganesyan, V., Kivelson, S. A. & Fradkin, E. Quantum theory of a nematic Fermi fluid. *Phys. Rev. B* **64,** 195109 (2001).
24. Yang, K.-Y., Rice, T. M. & Zhang, F.-C. Phenomenological theory of the pseudogap state. *Phys. Rev. B* **73,** 174501 (2006).
25. Stanescu, T. D. & Kotliar, G. Fermi arcs and hidden zeros of the Green function in the pseudogap state. *Phys. Rev. B* **74,** 125110 (2006).
26. Kyung, B. *et al.* Pseudogap induced by short-range spin correlations in a doped Mott insulator. *Phys. Rev. B* **73,** 165114 (2006).
27. Liang, R., Bonn, D. A. & Hardy, W. N. Preparation and X-ray characterization of highly ordered ortho-II phase $YBa_2Cu_3O_{6.50}$ single crystals. *Physica C* **336,** 57–62 (2000).
28. Liang, R., Bonn, D. A. & Hardy, W. N. Evaluation of CuO_2 plane hole doping in $YBa_2Cu_3O_{6+x}$ single crystals. *Phys. Rev. B* **73,** 180505 (2006).
29. Portugall, O. *et al.* The LNCMP: a pulsed-field user-facility in Toulouse. *Physica B* **346–347,** 668–672 (2004).

Supplementary Information is linked to the online version of the paper at www.nature.com/nature.

Acknowledgements We thank R. T. Brisson, G. G. Lonzarich, G. L. J. A. Rikken and A.-M. S. Tremblay for discussions, and M. Nardone and A. Audouard for their help with the experiment and analysis. We acknowledge support from the Canadian Institute for Advanced Research and the LNCMP, and funding from NSERC, FQRNT and a Canada Research Chair. Part of this work was supported by the French ANR IceNET and EuroMagNET.

Author Contributions N.D.-L. and C.P. contributed equally to this work.

Author Information Reprints and permissions information is available at www.nature.com/reprints. The authors declare no competing financial interests. Correspondence and requests for materials should be addressed to C.P. (proust@lncmp.org) or L.T. (louis.taillefer@physique.usherbrooke.ca).